Experimental Determination of an AUV's Drag Resistance in a Towing Tank

by

Leighton Hart-Kennedy

Submitted to the Department of Mechanical Engineering
in partial fulfillment of the requirements for the degree of

BACHELOR OF SCIENCE IN MECHANICAL AND OCEAN ENGINEERING
at the

MASSACHUSETTS INSTITUTE OF TECHNOLOGY

May 2024

Authored by: Leighton Hart-Kennedy
Department of Mechanical Engineering
May 10, 2024

Authored by: Michael Triantafyllou
Professor of Mechanical Engineering, Thesis Supervisor

Accepted by: Ken Kamrin
Professor of Mechanical Engineering
Undergraduate Officer, Department of Mechanical Engineering

Experimental Determination of an AUV's Drag Resistance in a Towing Tank

by

Leighton Hart-Kennedy

Submitted to the Department of Mechanical Engineering
on May 10, 2024 in partial fulfillment of the requirements for the degree of
BACHELOR OF SCIENCE IN MECHANICAL AND OCEAN ENGINEERING

ABSTRACT

The market for AUVs has expanded dramatically over the past several decades, a trend that is expected to continue over the next 10 years. AUVs operate autonomously using a dynamic controller that accounts for the dynamics of the system, including the drag resistance of the AUV. This paper examines the method of using a calm-water resistance test in a towing tank to determine the resistance of an AUV. A scale model of a survey class AUV was created using a 3d printer and mounted in a towing tank. The model was towed, and the resistance force recorded for a range from 0.3 to 0.9 m/s. An estimation of the AUV's resistance was determined using this data. The average drag coefficient was calculated at each speed using this data. The average drag coefficient was fit to a linear curve with the logarithm of the Reynolds number of the form $Cd = a * \log_{10} Re + b$ where $a = -0.0771 \pm 0.0507$ and $b = 0.484 \pm 0.277$.

ACKNOWLEDGMENTS

Thank you to Dr. Andrew Bennett and Professor Michael Triantafyllou at MIT Sea Grant for supporting me throughout this project.

CONTENTS

1. INTRODUCTION

Autonomous underwater vehicles (AUVs) are used by a wide variety of industries, including oil and gas, marine biology, and defense [1]. As technology improves, these vehicles are being used for tasks traditionally performed by human divers. AUVs can travel to regions of the ocean that human divers cannot reach, allowing them to perform a far broader scope of tasks. AUVs are incredibly versatile because they can be outfitted with a wide variety of sensors to record data. The popularity of AUVs has increased dramatically over the past several decades. A recent study valued the current global AUV market at $1.67 billion. That same study projected an annual growth rate of nearly 20% between 2023 and 2030 [2].

A thorough understanding of the specific dynamics of an AUV is incredibly important to the operation of that AUV. AUVs operate autonomously using a computer control scheme that accounts for the dynamics of the system. One important aspect of AUV dynamics is resistance. Previous literature on the estimation of AUV resistance focuses primarily on the use of Computational Fluid Dynamic (CFD) simulations of towing tank testing [3][4] and wind-tunnel testing [5].

This paper examines the method of using a calm-water resistance test in a towing tank to determine the resistance of an AUV. Calm-water resistance testing is the standard method of determining the resistance of surface ships. The resistance of a scale model of a survey class AUV was tested in a towing tank. An estimation of the AUV's resistance was determined using this data.

2. BACKGROUND

Autonomous Underwater Vehicles (AUVs)

Unmanned underwater vehicles are split into two classes: autonomous underwater vehicles (AUVs) and remotely operated vehicles (ROVs). The main difference between these two classes is that ROVs are in constant communication with an operator using a tether, while AUVs use on-board sensors to perform a pre-planned mission. Unlike ROVs, AUVs are not able to draw power from a surface power source. Inside an AUV, batteries store all the power that the AUV will have access to for the entire length of the planned mission. Power usage is one of the most important factors in designing an AUV. Therefore, AUVs often use a streamlined frame shape to minimize the resistance of the vehicle as it moves through the water. Figure 1 shows a popular AUV model that utilizes a streamlined hull shape. This paper deals with a survey class AUV developed to monitor coral reef bleaching.

Figure 1: Figure 1 shows a top view of the REMUS 100 AUV designed at Woods Hole Oceanographic Institution (WHOI). The REMUS series contains a number of different versions rated for different depths [6].

Surface Ship Resistance

In the latter half of the 19th century, William Froude devised a solution to the urgent problem of how to test a new ship design without building a full-scale model [7]. Froude discovered that the total resistance coefficient C_T of a ship could be separated into the frictional resistance C_F and the residuary resistance C_R, where C_F was a function of the Reynolds number and C_R was a function of the Froude number.

$$C_T = C_F(Re) + C_R(Fr)$$

The primary component of residuary resistance is wave-making resistance. When vessels travel along the surface of the water, they create Kelvin waves as shown in Figure 2 [7]. When waves are formed by the ship, less of the ship's energy is translated into forward motion. Ships do not only lose energy by creating waves. Ships also lose energy because they must traverse the waves generated at the bow.

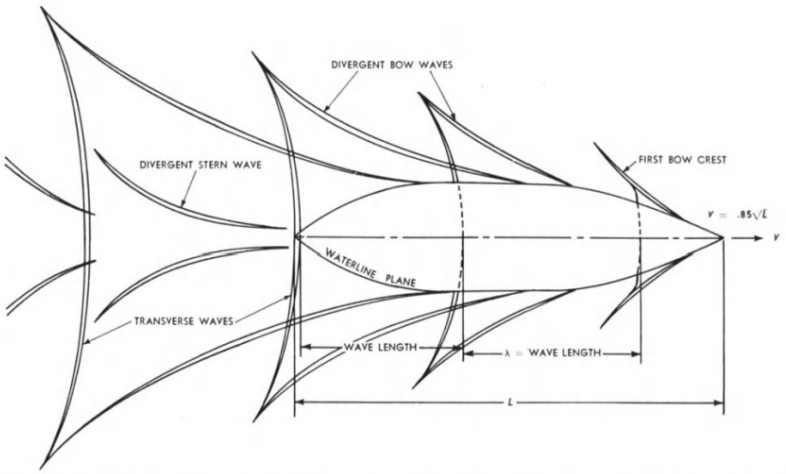

Figure 2: Diagram depicting the Kelvin waves produced by a displacement hull travelling at speed $v = 0.85\sqrt{L}$ where L is the length overall [7].

Froude designed a process for determining the total resistance of a ship by testing a scale model. In his process, Froude calculated the frictional resistance from the equivalent flat plate resistance and experimentally measured the total resistance in a towing tank. The residuary resistance of the scale model can be found by subtracting C_F from C_T. The residuary resistance of the full-size ship can be determined using only Froude similarity and the scale model residuary resistance.

Froude's experiments were performed using a towing tank. A towing tank is a large water basin used primarily for determining the properties of various marine vessels. A pair of rails are mounted above the basin and extend along the entire length of the tank. Models are attached to a towing carriage on the rails. One of the most common towing tank tests is a calm water resistance test, in which a model is towed at a constant speed and the forces on the model are measured. Today, towing tank tests are performed using a similar procedure to the process outlined by Froude over 100 years ago.

Determining the Resistance of an AUV

Determining the total resistance of an AUV is different from determining the total resistance of a surface ship because of the difference in residuary, or wave-making, resistance. As a ship's speed increases, wave-making resistance becomes the dominant resistance force. This force is the primary factor limiting the maximum speed of surface ships. When a ship is submerged, however, the surface waves generated by

forward movement decrease in amplitude with depth. At the typical depths used by AUVs, the wave-making resistance is approximately zero. The relationship between submerged depth and the wave-making resistance is shown in Figure 3.

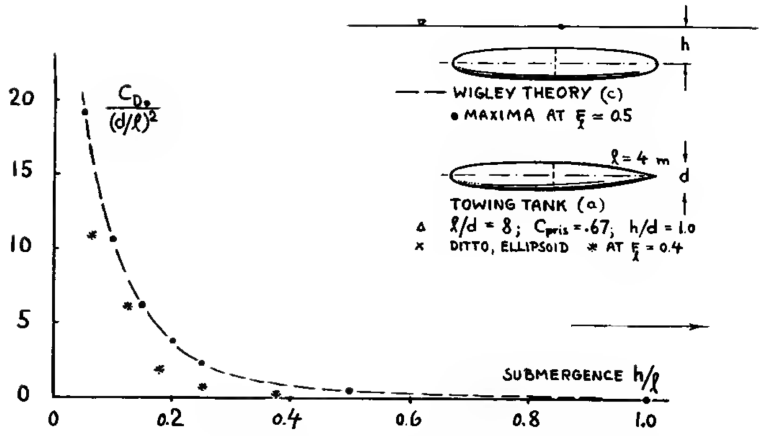

Figure 3: Figure 3 shows the wave-drag resistance coefficient for a streamlined body in a towing tank as the submergence increases. At depths greater than $5D$ (where D is the vessel's diameter), the wave-making resistance is near zero [8].

The dominant resistance forces on an AUV come from pushing water out of the way and from friction along the vessel's surface. These components are referred to as form drag and skin friction. Together these make up the total resistance. A diagram showing the relative scaling of form drag and skin friction with the vessel's length to diameter ratio is shown in Figure 4.

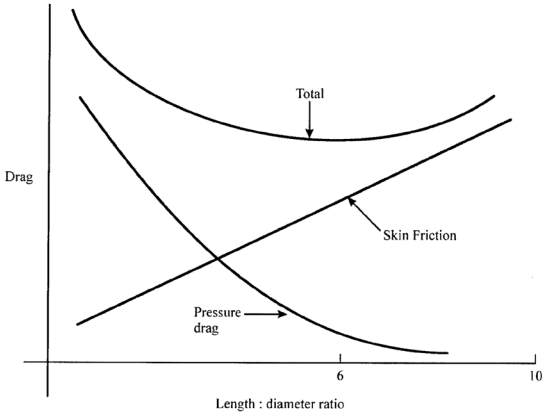

Figure 4: Figure 4 shows the relationship between form drag and skin friction as a vessel's length to diameter ratio increases [9].

For an AUV, we do not use Froude scaling to determine the resistance from a scale model because there is no wave-making resistance. The equation for the total resistance for an AUV is a function of the fluid density ρ, the resistance (or drag) coefficient C_d, the planform area $A = DL$, and the speed v.

$$R = \frac{1}{2}\rho C_d v^2 A$$

This equation can be rearranged to determine the drag coefficient at a given speed by measuring the force required to move the AUV at that speed at a constant rate.

$$C_d = \frac{F}{0.5\rho v^2 A}$$

This value scales with the Reynolds number differently depending on the geometry of the body. Figure 5 shows the drag coefficient scaling with Reynolds number for a variety of shapes.

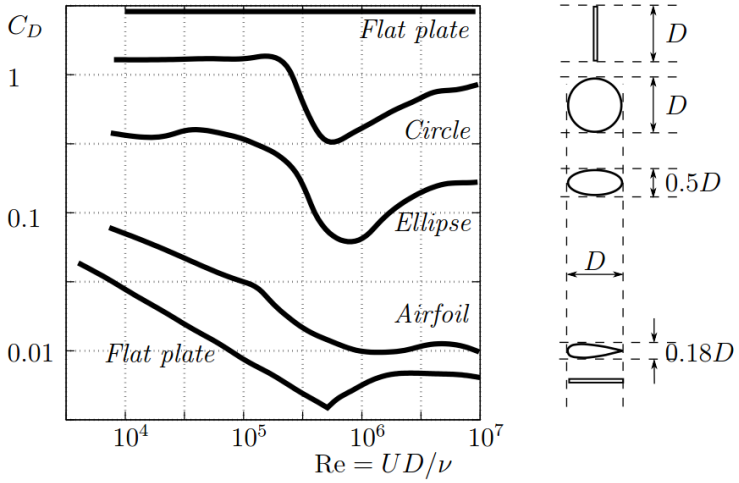

Figure 5: Figure 5 shows the relationship between the drag coefficient and the Reynolds number for a variety of shapes. The AUV in this paper is a streamlined shape and should therefore scale similarly to the airfoil [10].

3. EXPERIMENTAL DESIGN

The experiment was performed using a towing tank. A vertical strut used to mount models in the towing tank is attached to the bottom of the towing carriage. The towing carriage moves along a set of rails and measures the resistance force using a load cell as shown in Figure 6.

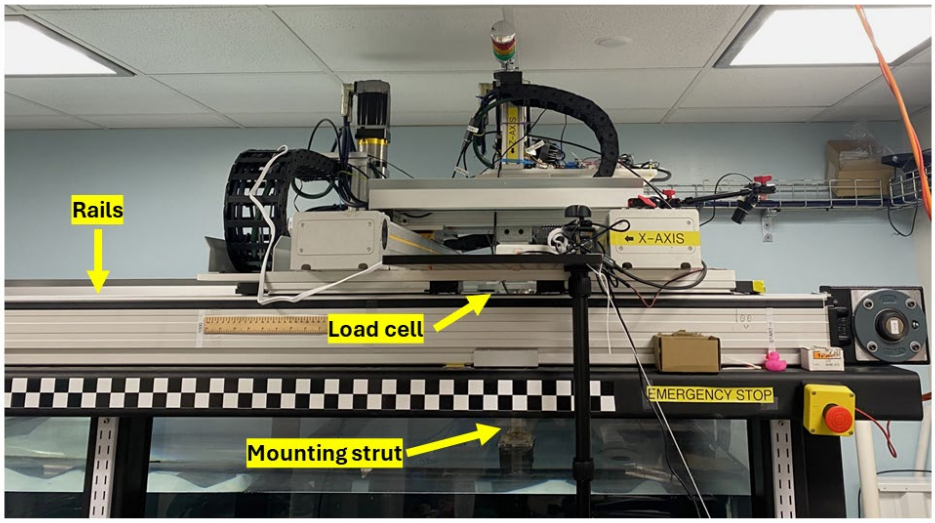

Figure 6: Diagram of the towing carriage. The AUV model attaches to the vertical strut, where it is pulled at a constant speed through the tank. The load cell records the resistance force in the transverse, longitudinal, and vertical directions.

A model of a survey class AUV was printed on a 3d printer at a 1:3 scale as seen in Figure 7a. A rectangular cut measuring 0.125" by 0.5" and extending vertically through the model was added to mount the model to the towing carriage. The model was mounted to a vertical strut using the rectangular slot. The vertical strut with the model was attached to the towing carriage. The model in the towing tank is shown in Figure 7b.

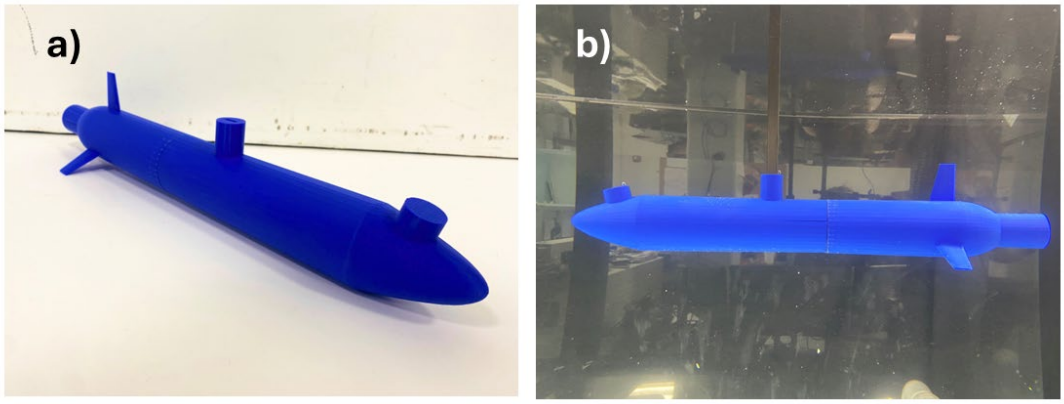

Figure 7: a) Figure 7a shows a scale model of the AUV's geometric shape. This model was printed at a 1:3 scale using a Bambu 3d printer. The model was printed in 2 parts and attached using plastic weld. b) Figure 7b shows the AUV inside the towing tank. The vertical strut hole is located near the center of mass.

The same process was followed for each trial. This process began with setting the desired speed for the trial run. The sensors were turned on and several seconds later the towing carriage started to move. This delayed start recorded several seconds of sensor noise at the start of each run to differentiate the sensor noise from the recorded force. During each trial, the model was carefully watched to check for any abnormal behavior. At a tow speed of 1 m/s, the model torqued around the mounting strut during the run, so the data from this run was removed from the dataset.

Sensors attached to the towing carriage record the force along the longitudinal, transverse, and vertical axis during the experiment. The model was towed at a constant speed through the tow tank and the data output was saved in MATLAB for analysis. After each run, a MATLAB figure of the data was generated. Based on this figure, data collected at speeds below 0.3 m/s was removed because the measured force was indistinguishable from the sensor noise.

This process was repeated for different towing speeds.

4. RESULTS AND DISCUSSION

After gathering data of the resistance force at a variety of speeds, the resistance force was calculated using the force measured in the longitudinal (or x) direction. The data from the trials at speeds 0.1 m/s, 0.2 m/s, and 1 m/s were removed from the dataset as described in Section 3. For each trial, the data was trimmed to only include the forward movement section of the trial (removing the stationary period at the beginning and the backwards movement of the model). The force data from speeds of 0.3 m/s to 0.9 m/s is shown in Figure 8 with a line representing the average force plotted over the data.

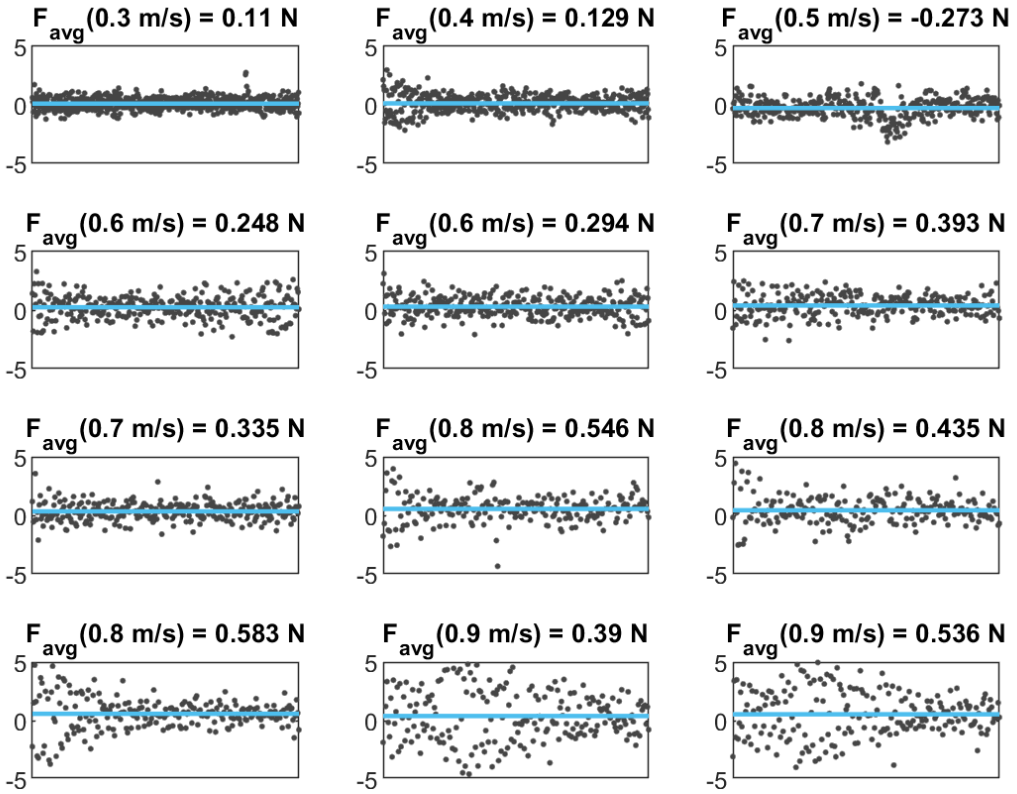

Figure 8: The data collected, excluding the speeds where sensor readings were not distinguishable from the sensor noise. A line showing the average force for each run is plotted over the data.

The drag coefficient was calculated for each run using the equation $C_d = \frac{F}{0.5\rho v^2 A}$. Key dimensions of the model are shown below in Table 1. The density of the freshwater in the tank was assumed to be 1000 kg/m^3.

Table 1: Selected Model Parameters

Length	0.460 m
Diameter	0.056 m
Planform Area	0.0258 m^2

The resulting drag coefficients for each run are plotted in Figure 9 with the average drag coefficient plotted on top of the data.

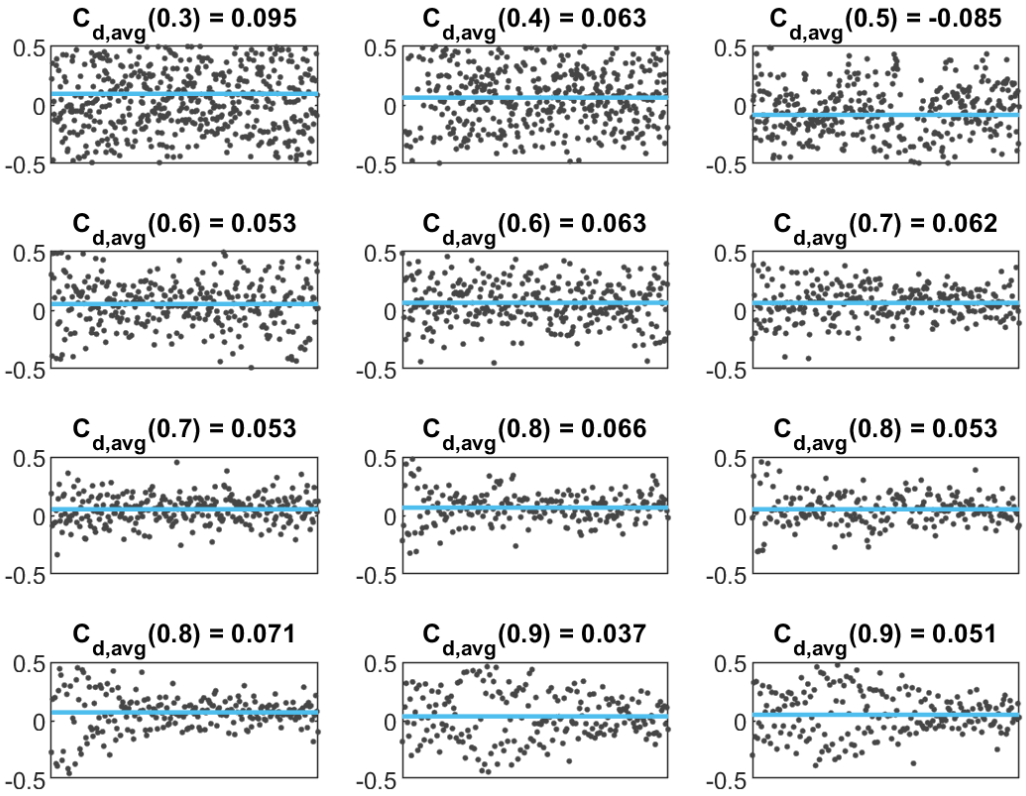

Figure 9: The calculated resistance coefficient for each trial run. A line showing the average drag coefficient for each run is plotted over the data.

For a streamlined shape, the drag coefficient scales roughly linearly with the logarithm of the Reynolds number in the range $10^4 < Re < 10^6$. The drag coefficient was plotted against the Reynolds number with the Reynolds number using a logarithmic axis. The Reynolds number was calculated using $Re = \frac{\rho v L}{\mu}$. The length was chosen over the diameter because the skin friction dominates at this length to diameter ratio.

Using the data, an equation for the drag coefficient as a function of the Reynolds number was created by fitting a curve to the data. The curve is given by the equation $Cd = a * \log_{10} Re + b$ where $a = -0.0771 \pm 0.0507$ and $b = 0.484 \pm 0.277$. The data and curve fit are shown in Figure 10.

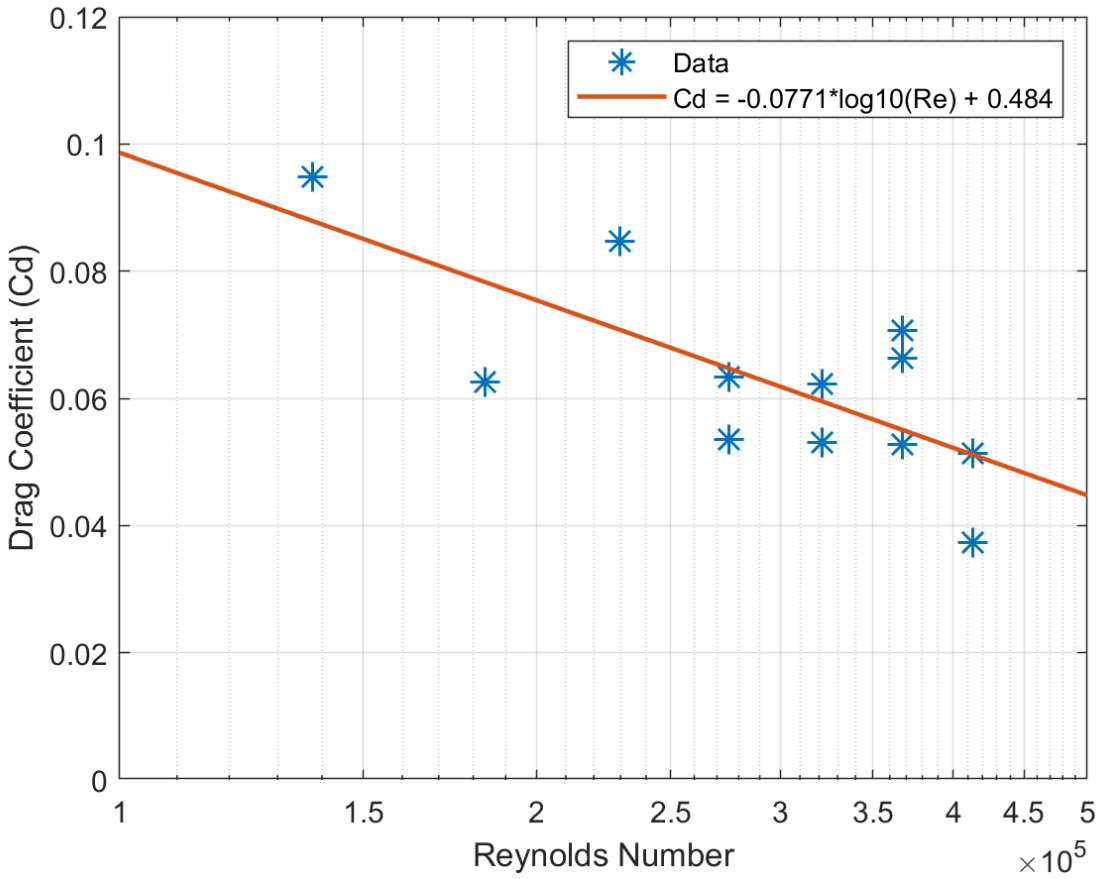

Figure 10: The calculated resistance coefficient is plotted against the Reynolds number. The data is fit to a curve of the form $Cd = a * \log_{10} Re + b$ where $a = -0.0771 \pm 0.0507$ and $b = 0.484 \pm 0.277$. Each data point corresponds to the average frag coefficient from one trial in the towing tank.

5. CONCLUSIONS

The relationship between the Reynolds number and drag coefficient for a small survey-class AUV was analyzed. As the Reynolds number increased, the drag coefficient of the model decreased. The drag coefficient was determined to have a linear relationship with the logarithm of the Reynolds number. For

this specific AUV, the relationship is given by $Cd = a * \log_{10} Re + b$ where $a = -0.0771 \pm 0.0507$ and $b = 0.484 \pm 0.277$.

Based on the results of this experiment, a towing tank is a simple and effective way to determine the drag coefficient of an AUV over a range of Reynolds numbers. However, the sensors used in the towing tank should be chosen carefully due to the large impact of sensor noise on the data. The results of this experiment are limited by the small sample size. Only one model of AUV was tested in a towing tank, and the limitations of the load cell and towing tank restrained the possible carriage speeds used in this experiment.

The applicability of the model drag coefficient to the full-size AUV will be the subject of further research. After the full-size model has been completed, the procedures outlined in this paper will be repeated and the resulting drag coefficient curves can be compared.

REFERENCES

[1] Trembanis, A. C., Lundine, M., & McPherran, K. (2021). Coastal Mapping and Monitoring. *Encyclopedia of Geology (2nd ed), 251–266.* https://doi.org/10.1016/b978-0-12-409548-9.12466-2

[2] *Autonomous Underwater Vehicle (AUV) Market projected to reach USD 5.86 Billion by 2030, growing at a CAGR of 19.6% during the forecast period of 2023-2030 - pronounced by MarketDigits in its recent study*. (2024, January 9). GlobeNewswire. https://www.globenewswire.com/news-release/2024/01/09/2806512/0/en/Autonomous-Underwater-Vehicle-AUV-Market-projected-to-reach-USD-5-86-Billion-by-2030-growing-at-a-CAGR-of-19-6-during-the-forecast-period-of-2023-2030-pronounced-by-MarketDigits-in.html

[3] Phillips, A., Furlong, M., & Turnock, S. R., (2007, September 17). The Use of Computational Fluid Dynamics to Assess the Hull Resistance of Concept Autonomous Underwater Vehicles. *OCEANS 2007 – Europe*. https://doi.org/10.1109/OCEANSE.2007.4302434

[4] Javanmard, E., & Mansoorzadeh, S. (2019). A Computational Fluid Dynamics Investigation on the Drag Coefficient Measurement of an AUV in a Towing *Tank. Journal of Applied Fluid Mechanics, Vol. 12, No. 3*, pp. 947-959. https://doi.org/10.29252/jafm.12.03.29525

[5] Sulisetyono, A., & Wardhana, R. (2022, December). The Resistance Evaluation of the Autonomous Underwater Vehicle (AUV) Using the Low Speed Wind Tunnel Test. *Journal of Engineering Science and Technology, Vol. 17, No. 6,* 4355 – 4366.

[6] *REMUS 100.* (n.d.). Woods Hole Oceanographic Institution. https://www2.whoi.edu/site/osl/vehicles/remus-100/

[7] Gillmer, T. C., Johnson, B. (1985). *Introduction to naval architecture.* Naval Institute Press.

[8] Hoerner, S. F. (1965). *Fluid-dynamic drag: Practical information on aerodynamic drag and hydordynamic resistance*. The Author.

[9] Moonesun, M., Javadi, M., Charmdooz, P., Karol, & Mikhailovich, U. (2013). Evaluation of submarine model test in towing tank and comparison with CFD and experimental formulas for fully submerged resistance. *Indian Journal of Geo-Marine Sciences. 42.* 1049-1056.

[10] *Overview of common fluid flow phenomena.* (n.d.). Flow Illustrator. http://www.flowillustrator.com/fluid-dynamics/overview-of-common-fluid-flow-phenomena.php